Journal of Magnetism and Magnetic Materials ▮ (▮▮▮▮) ▮▮▮–▮▮▮

Contents lists available at ScienceDirect

Journal of Magnetism and Magnetic Materials

journal homepage: www.elsevier.com/locate/jmmm

Influence of growth morphology on the Néel temperature of CrRu thin films and heterostructures

A.R.E. Prinsloo [a,*], H.A. Derrett [a], O. Hellwig [b], E.E. Fullerton [c], H.L. Alberts [a], N. van den Berg [d]

[a] Department of Physics, University of Johannesburg, P.O. Box 524, Auckland Park, Johannesburg 2006, South Africa
[b] San Jose Research Center, Hitachi Global Storage Technologies, 3403 Yerba Buena Road, San Jose, CA 95135, USA
[c] University of California, San Diego, La Jolla, CA, USA
[d] Department of Physics, University of Pretoria, Lynwood road, Pretoria, South Africa

ARTICLE INFO

Keywords:
Cr alloy
Epitaxial thin film
Heterostructure
Spin density wave
Electrical resistivity

ABSTRACT

Dimensionality effects on epitaxial and polycrystalline $Cr_{1-x}Ru_x$ alloy thin films and in Cr/Cr–Ru heterostructures are reported. X-ray analysis on $Cr_{0.9965}Ru_{0.0035}$ epitaxial films indicates an increase in the coherence length in growth directions (1 0 0) and (1 1 0) with increasing thickness (d), in the range $20 \le d \le 300$ nm. Atomic force microscopy studies on these films shows pronounced vertical growth for $d > 50$ nm, resulting in the formation of columnar structures. The Néel temperatures (T_N) of the $Cr_{0.9965}Ru_{0.0035}$ films show anomalous behaviour as a function of d at thickness $d \approx 50$ nm. It is interesting to note that this thickness corresponds to that for which a change in film morphology occurs. Experiments on epitaxial $Cr_{1-x}Ru_x$ thin films, with $0 \le x \le 0.013$ and $d = 50$ nm, give T_N–x curves that correspond well with that of bulk $Cr_{1-x}Ru_x$ alloys. Studies on $Cr/Cr_{0.9965}Ru_{0.0035}$ superlattices prepared on MgO(1 0 0), with the Cr layer thickness varied between 10 and 50 nm, keeping the $Cr_{0.9965}Ru_{0.0035}$ thickness constant at 10 nm, indicate a sharp decrease in T_N as the Cr separation layers reaches a thickness of 30 nm; ascribed to spin density wave pinning in the Cr layers for $d < 30$ nm by the adjacent CrRu layers.

1. Introduction

Cr and Cr alloys with their spin density wave (SDW) antiferromagnetism, exhibit a richness of magnetic phenomena that have attracted considerable interest for many years [1]. Bulk Cr is an itinerant electron antiferromagnetic material that forms an incommensurate SDW (ISDW) phase below its Néel temperature $T_N = 311$ K [1]. The ISDW period varies from 78 Å at T_N to 60 Å at 10 K [2,3]. Thin films and heterostructures of Cr and Cr alloys show fascinating properties, not observed in the bulk [3,4], including the mediating role of Cr thin films in exchange coupled superlattices and in giant magnetoresistive (GMR) materials [2].

For the bulk $Cr_{1-x}Ru_x$ alloy system a commensurate SDW (CSDW) phase is induced at a critical concentration $x_L \approx 0.002$ and T_N of the CSDW-paramagnetic Néel transition rises rapidly for $x > x_L$. CSDW $Cr_{1-x}Ru_x$ alloys show outstanding magnetic properties, such as exceptionally large concentration and pressure derivatives of T_N and peculiar magnetoelastic properties, that have been studied extensively in bulk alloys containing $x = 0.003$ [5–7]. Extending studies to Cr–Ru alloy thin films will lead to significant innovation regarding the role of dimensionality and microstructure effects on the properties of this alloy system. In this paper, we report on dimensionality effects on epitaxial and polycrystalline $Cr_{1-x}Ru_x$ alloy monolayer thin films, as well as on epitaxial $Cr/Cr_{0.9965}Ru_{0.0035}$ superlattices.

2. Experimental techniques

The Cr–Ru films were prepared using DC magnetron cosputtering at 800 °C from elemental sources onto single-crystal MgO(1 0 0), *a*-plane sapphire and polycrystalline quartz substrates. Films were prepared in a thickness series of fixed concentration Cr+0.35 at% Ru with thickness, d, varying between 20 and 300 nm; as well as in a $Cr_{1-x}Ru_x$ concentration series with x in the range $0 \le x \le 0.013$ and thickness fixed at 50 nm. $Cr/Cr_{0.9965}Ru_{0.0035}$ superlattices were grown using magnetron sputtering onto MgO(1 0 0) substrates. A 10 nm Cr buffer layer was first deposited at 800 °C and then the superlattices were deposited at 400 °C. The $Cr_{0.9965}Ru_{0.0035}$ layers were cosputtered from elemental sources and the layer thickness was held constant at 10 nm. The Cr layer thickness (t_{Cr}) was fixed at 10, 20, 30, 40 or 50 nm for each superlattice. Superlattice samples were prepared to a total thickness of 700 nm. The concentrations and thicknesses of the films and heterostructures were confirmed

* Corresponding author. Tel.: +27 11 559 2346; fax: +27 11 559 2339.
E-mail address: alettap@uj.ac.za (A.R.E. Prinsloo).

0304-8853/$ - see front matter © 2009 Elsevier B.V. All rights reserved.
doi:10.1016/j.jmmm.2009.07.063

using Rutherford Back Scattering techniques. Atomic force microscopy (AFM) imaging was used to study the topographic properties of the CrRu thin films and the film structure was characterized using X-ray diffraction (XRD) techniques. Electrical resistance measurements, using standard DC four-probe methods, were employed to determine the Néel transition temperatures for these samples.

3. Results and discussion

The XRD measurements indicate that all the films prepared on MgO(1 0 0) and *a*-plane sapphire, are epitaxial and exhibit a single crystallographic orientation, with the Cr and Cr–Ru showing preferred growth directions of (1 0 0) and (1 1 0) for the respective substrates. Typical examples of XRD measurements are shown in Fig. 1. The samples prepared on quartz were polycrystalline. The full-width at half-maximum (FWHM) of the Bragg peaks was used to determine the length scale (in growth direction) over which the film is structurally coherent [8]. Analysis on $Cr_{0.9965}Ru_{0.0035}$ thin films of thicknesses in the range $10 \le d \le 300$ nm, grown on MgO(1 0 0) and *a*-plane sapphire substrates, indicate that the crystal coherence length in growth directions (1 0 0) and (1 1 0), respectively, of the films increased with increasing *d*. Results obtained for the $Cr_{0.9965}Ru_{0.0035}$ thickness series are summarized in Table 1, where the Debye–Scherrer formula was used in the calculation of the coherence lengths after removing the instrument resolution.

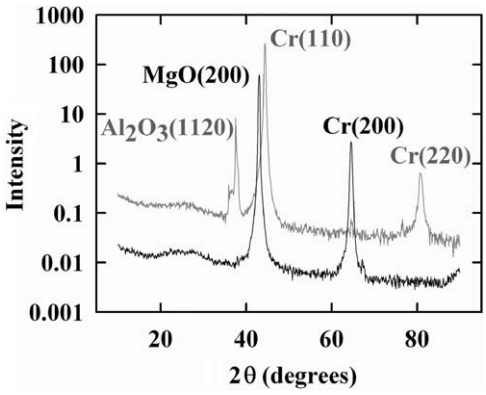

Fig. 1. $\theta-2\theta$ XRD scans, with the scattering vector normal to the plane of the film, for the $Cr_{0.9965}Ru_{0.0035}$ thin films of thickness 100 nm prepared, respectively, on MgO(1 0 0) (black) and *a*-plane sapphire (grey) substrates.

The mosaic spread was determined from the FWHM of the rocking curve [8]. For $Cr_{0.9965}Ru_{0.0035}$ thin films prepared on MgO(1 0 0) substrates (Table 1) a general decrease in mosaicity with increasing thickness is observed, except for the film of thickness 100 nm that does not fit into this pattern, with a mosaicity of 0.94°. In the cases of films of thickness 10 and 25 on MgO(1 0 0) in Table 1 the mosaicity exceeds 1°, while the films of thicknesses 50, 150 and 300 nm show mosaicity in the range 0.37–0.61°. This indicates a general trend of improved crystal quality with films thickness [4,8]. On the other hand the mosaicities of $Cr_{0.9965}Ru_{0.0035}$ films prepared on *a*-plane sapphire are all smaller than 0.35° (Table 1), indicating a high degree of crystallographic alignment.

In case of $Cr_{1-x}Ru_x$ thin films, with *x* in the range $0 \le x \le 0.013$ and of fixed thickness 50 nm, the coherence length was observed to be approximately independent of *x*, being about 30 and 40 nm for MgO(1 0 0) and *a*-plane sapphire, respectively. The mosaicity of these films indicated no specific trends with increasing Ru concentration, and stays approximately constant at 0.6° and 0.2° for MgO(1 0 0) and *a*-plane sapphire, respectively.

Comparisons of in- and out-of-plane XRD scans on representative samples indicate an out-of-plane strain of approximately 0.4% in the layers prepared on MgO(1 0 0), while no strain was observed within the detection limit in those prepared on *a*-plane sapphire. XRD scans on the $Cr/Cr_{0.9965}Ru_{0.0035}$ superlattices prepared on MgO(1 0 0) confirmed (1 0 0) growth with crystalline coherence lengths of approximately 40 nm and mosaic spread less than 0.6°.

AFM studies on the $Cr_{0.9965}Ru_{0.0035}$ monolayer thickness series indicate that epitaxial films with $d = 10$ nm have homogeneous, smooth surface morphology. As *d* increases, grains become visible in the AFM images, with an increase in grain size together with pronounced vertical growth, resulting in the formation of columnar structures for $d > 50$ nm. This is depicted in Fig. 2 for the example of the $d = 150$ nm film prepared on MgO(1 0 0). AFM studies on the $Cr_{1-x}Ru_x$ concentration series indicate, for growth on all three substrates, an increase in grain size as the Ru concentration is increased. For instance for growth on MgO(1 0 0) the grain size increased from 3.3 to 9.7 nm on increasing *x* from 0.0022 to 0.013.

The Néel temperatures (T_N) of the films were determined from anomalies observed in electrical resistance (*R*) measurements as a function of temperature (*T*). An example of the *R*–*T* curves determined for the $Cr_{0.9965}Ru_{0.0035}$ sample of thickness 50 nm on

Table 1
The measured out-of-plane full-width at half-maximum (FWHM) XRD parameters of the selected Bragg peak and the mosaic spread of this peak, for epitaxial $Cr_{0.9965}Ru_{0.0035}$ films of thickness *d* prepared at 800 °C on MgO(1 0 0) and *a*-plane sapphire substrates, respectively. The coherence length, T_{coh}, was calculated using the Debye–Scherrer equation after removing the resolution of the instrument.

d (nm)	MgO(1 0 0)			*a*-plane sapphire		
	FWHM (2 0 0)	T_{coh} (nm)	Mosaic (2 0 0)	FWHM (1 1 0)	T_{coh} (nm)	Mosaic (1 1 0)
10	1.06°	9	1.54°	0.82°	10	0.13°
25	0.50°	20	1.17°	0.34°	25	0.16°
50	0.33°	30	0.61°	0.23°	39	0.28°
100	0.37°	27	0.94°	0.25°	36	0.34°
150	0.26°	38	0.37°	0.20°	45	0.31°
300	0.26°	38	0.37°	0.18°	50	0.32°

Please cite this article as: A.R.E. Prinsloo, et al., J. Magn. Magn. Mater. (2009), doi:10.1016/j.jmmm.2009.07.063

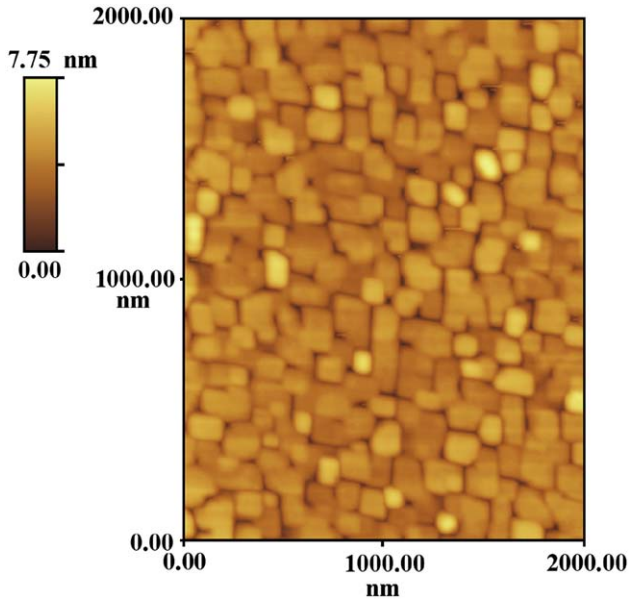

Fig. 2. AFM image of a $Cr_{0.9965}Ru_{0.0035}$ thin film of thickness 150 nm prepared on MgO(1 0 0).

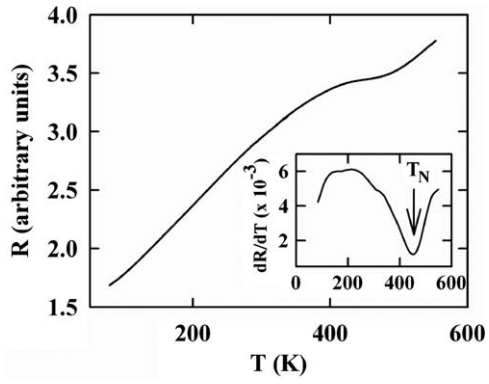

Fig. 3. Resistance (R) versus temperature (T) graph for a $Cr_{0.9965}Ru_{0.0035}$ thin film of thickness 50 nm prepared on a-plane sapphire. The inset shows dR/dT versus T, where the temperature of the minimum was taken as the Néel temperature (T_N).

a-plane sapphire, is shown in Fig. 3. T_N was taken at the inflection point on the R–T curves, determined by the minimum in the dR/dT curve shown in the inset. This is one of the accepted methods generally used for the determination of T_N in Cr based thin films [9]. It should however be mentioned that extrinsic morphology contributions that dramatically change the resistance may bias obtained T_N values to some extent. The variation in T_N with layer thickness in the $Cr_{0.9965}Ru_{0.0035}$ thickness series is shown in Fig. 4 for the three substrates used. For the epitaxial $Cr_{0.9965}Ru_{0.0035}$ thin films (Fig. 4 (a) and (b)) T_N peaks fairly sharply at $d \approx 50$ nm for growth on both MgO(1 0 0) and a-plane sapphire substrates. Anomalous behaviour is also observed for polycrystalline $Cr_{0.9965}Ru_{0.0035}$ films, grown on polycrystalline quartz (Fig. 4 (c)), for which a sharp decrease of about 30 K in T_N is observed between $d = 50$ and 100 nm. It is interesting to note that the thickness $d \approx 50$ nm of the anomalous T_N–d behaviour of Fig. 4, corresponds to that for which a change in morphology is observed in the AFM studies.

T_N–x curves obtained for the $Cr_{1-x}Ru_x$ concentration series, of constant film thickness $d = 50$ nm, are shown in Fig. 5 for the three substrates. The epitaxially grown films (Fig. 5 (a) and (b)) display initial sharp increases in T_N, starting at $T_N \approx 310$ K for $x = 0$, which is close to the value for bulk Cr, and then tend to level off.

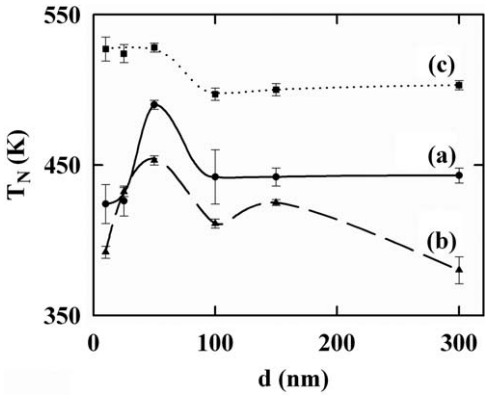

Fig. 4. The Néel temperature (T_N) of the $Cr_{0.9965}Ru_{0.0035}$ thickness series as a function of thickness (d) for samples prepared on (a) MgO(1 0 0) , (b) a-plane sapphire and (c) polycrystalline quartz. The lines are guides to the eye.

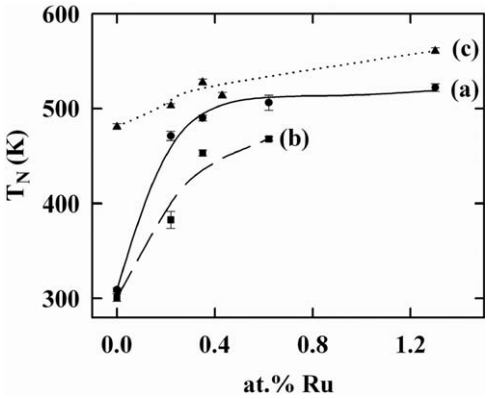

Fig. 5. The Néel temperature (T_N) as a function of Ru concentration for the $Cr_{1-x}Ru_x$ concentration series prepared on (a) MgO(1 0 0), (b) a-plane sapphire and (c) polycrystalline quartz. The lines are guides to the eye.

This behaviour is very similar to what is observed for bulk $Cr_{1-x}Ru_x$ alloys [1]. The polycrystalline films (Fig. 5 (c)) behave however differently, showing $T_N \approx 480$ K for $x = 0$, and increases only relatively little with increasing x, quite different from the bulk behaviour. The high T_N for $x = 0$ is unexpected and of unknown origin, but incidentally corresponds with $T_N = 475$ K for the CSDW-P Néel transition induced in bulk Cr through stresses associated with cold working [10]. Previous studies [11] on polycrystalline Cr films, grown on Corning glass substrates, also show significant enhancement, up to 60 K above the bulk value, in T_N for $d \leq 30$ nm. This is ascribed to internal tensile stresses in the films that arise, in part, from the grain boundaries [12,13]. It is then possible that the polycrystalline films with a high density of grain boundaries may behave like a cold worked sample, resulting in a high temperature CSDW-P transition for the Cr film on quartz [13], where as the epitaxial films will have different internal stresses.

Resistivity studies on $Cr/Cr_{0.9965}Ru_{0.0035}$ superlattices prepared on MgO(1 0 0), with the Cr layer thickness, t_{Cr}, varied between 10 and 50 nm, keeping the $Cr_{0.9965}Ru_{0.0035}$ thickness constant at 10 nm, indicate a sharp decrease in T_N as the Cr separation layers reaches a thickness of about 20–30 nm, shown in Fig. 6. This may be ascribed [3,14–16] to proximity magnetism. The Ru doping creates a high T_N $Cr_{0.9965}Ru_{0.0035}$ layer of thickness 10 nm that orders in a CSDW phase below $T_N \approx 420$ K (Fig. 4 (a)). For $t_{Cr} < 30$ nm, the adjacent high T_N CSDW CrRu layers induce magnetic ordering in the Cr layer to temperatures much greater than that normally observed for pure Cr resulting in a single phase

Please cite this article as: A.R.E. Prinsloo, et al., J. Magn. Magn. Mater. (2009), doi:10.1016/j.jmmm.2009.07.063

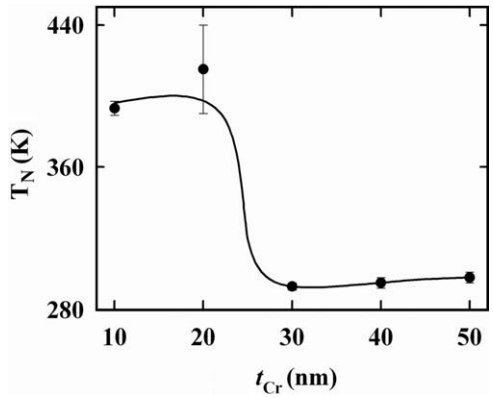

Fig. 6. The Néel temperature (T_N) as a function of Cr layer thicknesses (t_{Cr}) for the $Cr/Cr_{0.9965}Ru_{0.0035}$ heterostructures prepared on MgO(1 0 0). The line is a guide to the eye.

transition. In superlattices with $t_{Cr} > 30$ nm, the effect of the $Cr_{0.9965}Ru_{0.0035}$ layers on the Cr Néel transition temperature subsides and separate phase transitions are expected. However, for $t_{Cr} \geq 30$ nm the amount of Cr material in the multi-layer system may become large enough, presumably to such an extent that its effect on T_N dominates, thereby masking the Néel transition in the Cr–Ru layers. This will result in only one ordering temperature, that of bulk Cr, as is observed. What is unique in this system, when compared to earlier studies [15,16], is that the transition from a single transition to expected independent transitions occurs at roughly an order of magnitude larger layer thicknesses. This most likely results from the itinerant nature of the Cr/Cr–Ru systems compared to the local moment $FeF_2/CoFe_2$ [15] and NiO/CoO [16] systems previously studied.

4. Conclusions

Interesting correlations were found between layer thickness, morphology and magnetic properties of $Cr_{0.9965}Ru_{0.0035}$ thin films; indicating 50 nm to be a critical thickness. Epitaxial $Cr_{1-x}Ru_x$, with $0 \leq x \leq 0.013$, prepared at this critical thickness show behaviour similar to that of bulk material. Resistivity studies on $Cr/Cr_{0.9965}Ru_{0.0035}$ superlattices suggest proximity induced magnetism in the Cr layers for $t_{Cr} < 30$ nm. In order to fully understand the behaviour of Cr in this superlattice arrangement, the present results should be supplemented by neutron diffraction studies.

Acknowledgement

This work is supported by the South African NRF (Project 61388).

References

[1] E. Fawcett, H.L. Alberts, V. Yu Galkin, D.R. Noakes, J.V. Yakhmi, Rev. Mod. Phys. 66 (1994) 25.
[2] H.J. Zabel, J. Phys.: Condens. Matter 11 (1999) 9303.
[3] E.E. Fullerton, J.L. Robertson, A.E.R. Prinsloo, H.L. Alberts, S.D. Bader, Phys. Rev. Lett. 91 (2003) 237201.
[4] R.K. Kummamuru, Y.A. Soh, Nature 452 (2008) 859.
[5] H.L. Alberts, A.H. Boshoff, J. Magn. Magn. Mater. 104-107 (1992) 2031.
[6] H.L. Alberts, J.A.J. Lourens, J. Phys. F 18 (1988) L213.
[7] M. Cankurtaran, G.A. Saunders, Q. Wang, P.J. Ford, H.L. Alberts, Phys. Rev. B 46 (1992) 1157.
[8] J.E. Mattson, E.E. Fullerton, C.H. Sowers, S.D. Bader, J. Vac. Sci. Technol. A 13 (2) (1995) 276.
[9] J.E. Mattson, B. Brurnitt, M.B. Brodsky, J.B. Ketterson, J. Appl. Phys. 67 (9) (1990) 4889.
[10] E. Fawcett, Rev. Mod. Phys. 60 (1988) 209.
[11] J.A.J. Lourens, S. Arajs, H.F. Helbig, L. Cherlet, E.A. Mehanna, J. Appl. Phys. 63 (1988) 4282.
[12] H. Windischmann, Crit. Rev. Solid State Mater. Sci. 17 (1992) 547.
[13] Z. Boekelheide, E. Helgren, F. Hellman, Phys. Rev. B 76 (2007) 224429.
[14] R.W. Wang, D.L. Mills, Phys. Rev. B 46 (1992) 11681.
[15] C.A. Ramos, D. Lederman, A.R. King, V. Jaccarino, Phys. Rev. Lett. 65 (1990) 2913.
[16] E.N. Abarra, K. Takano, F. Hellman, A.E. Berkowitz, Phys. Rev. Lett. 77 (1996) 3451.